Desalination and Water Treatment
www.deswater.com
doi: 10.5004/dwt.2022.29108

279 (2022) 195–202
December

Preparation and characterization of biosorbent of shrimp co products-based and its potential application in the removal of an anionic dye

Nedjma Khelifa[a,c,*], Souhila Aithamoudi[b], Nadia Aicha Laoufi[c]

[a]*Ecole Nationale Supérieure des Sciences de la Mer et de l'Aménagement du Littoral, BP 19, bois des cars, Dely Ibrahim, Algiers, Algeria, Tel. +213559340999; email: khelifa_nedj@yahoo.fr*
[b]*Centre de Recherche Scientifique et Technique en Analyses Physico – Chimiques, BP 384, Siège ex-Pasna Zone Industrielle Bou-Ismail, 42004 Tipaza. Algeria*
[c]*Laboratoire des Phénomènes de Transfert, Département de Génie Chimique et de Cryogénie. U.S.T.H.B. Faculté GM&GP Bp 32, El Alia, 16111 Bab Ezzouar, Algiers, Algeria*

Received 30 June 2022; Accepted 29 September 2022

ABSTRACT

A biosorbent material was prepared from a shrimp co-product (SCP) collected from local fishery (Algiers, Algeria), following a simple route needing only washing, drying and grinding at room temperature, without any chemical addition. The SCP biosorbent was characterized via X-ray diffraction, Fourier-transform infrared spectroscopy and scanning electron microscopy-energy-dispersive X-ray spectroscopy (SEM-EDX) techniques. The results indicated that SCP consisted mostly of calcium carbonate. SEM images revealed the presence of cavities more or less homogeneous, with different geometries. The biosorption study selected for the removal of Congo red (CR) dye gave a maximum experimental biosorption capacity of 25.628 mg/g. Several models were used to fit the biosorption experiment. The mono-layer biosorption was confirmed by the good fit of the Langmuir model with experimental data. The biosorption kinetic followed the pseudo-second-order model involving a chemical biosorption process. The SCP was proven to be a potentially sustainable biosorbent for dyes retention.

Keywords: Shrimp co-products; Biosorbent; Characterization; Biosorption; Congo red

1. Introduction

Human societies since their origin have exploited and altered the physical and biological environment in various aspects. Due to this impact and in order to attenuate the effect, durable biomaterials are in demand. However, the synthetic dyes are both toxic and no biodegradable [1]. Such dyes are used in the industries of textiles and leather dyeing, as well as printing, pharmaceuticals [2–5]. Generally, dyes are divided into chemical structures such as anionic, cationic and non-ionic. Anionic reactive dyes are both stable and light resistant [6]. Dyes must be removed once used to avoid marine ecosystem pollution [7,8].

The treatment of waste water has been achieved by various techniques such as filtration [9], flotation [10], photocatalysis [11], biological [12], ion exchange and advanced oxidation [13], adsorption [14–16].

Adsorption is commonly used due to the simplicity of the process and its lower involved cost compared to other processes [17,18]. Therefore, considerable efforts are devoted to the removal of organic contaminants [19,20] by using low-cost renewable adsorbents as an alternative to expensive fossil activated carbons [21–23]. The cost of the adsorbent is an important parameter to be considered as well as other performance indicators related to environmental impacts.

* Corresponding author.

Presented at the First International Congress of Energy and Industrial Process Engineering (ICEIPE'22) 23–25 May 2022, Algiers, Algeria

Hence, there is a growing research of bio-based adsorbents to address the pollution issue.

A varied range of by-products can be obtained from shrimp co-products [24,25], yet processing plants continue to release considerable quantities of these co-products into the environment as waste products. For this reason, more in-depth studies are needed on shrimp co-products-based physical and chemical properties. We propose to use recovered shrimps waste by-products to use as feedstock in the preparation of dye adsorbent materials. In previous studies [26–29], an adsorbent extracted from shrimp waste (chitosan) has been used for the removal of heavy metals [26] antibiotics [27], oil [28] and dye [29].

The study of potential adsorbent of marine co product in the adsorption of pollutants has recently started [30]. Agricultural and industrial waste materials have been studied as alternative feedstock to remove dyes and other pollutants [31].

In this study a biosorbent was prepared from co-products from shrimp. Following washing step, shrimp shells were dried and grinding then the powder was characterized via X-ray diffraction (XRD), Fourier-transform infrared spectroscopy (FTIR) and scanning electron microscopy-energy-dispersive X-ray spectroscopy (SEM-EDX) techniques. Removal of Congo red (CR) dye on this novel biosorbent using adsorption kinetics and equilibrium isotherm was investigates. Another goal is to study equilibrium data using mathematical models. Characteristics of the intra particular diffusion, pseudo-first and second-order models and the Langmuir, Freundlich and Redlich–Peterson isotherms were evaluated using nonlinear regression models.

2. Material and method

2.1. Preparation of shrimp co-products powder

Shrimp shells collected from a local fishery (Algiers, Algeria) washed several times with water then with a solution of hydrochloric acid (10^{-3} N), dried in a ventilated oven at (40°C) over night, crushed and finally stored in airtight glass bottles for further experiments. This powder will be put back in the oven at 105°C for 24 h just before use.

2.2. Preparation of aqueous Congo red solution

Congo red (CR) is an anionic dye (Fig. 1). Solutions of the dye CR were analyzed by UV Visible at its adsorption wavelength (λ_{max} = 498 nm). CR stock-solution (1 g/L) were prepared by shaking in distilled water and kept at room temperature. The 50 mg/L solution used in the study is prepared by dilution of a quantity of the 1 g/L stock solution.

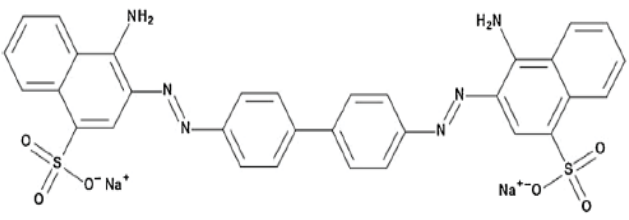

Fig. 1. Molecular structure of Congo red.

2.3. Characterization of material used

The biosorbent characterization was performed using different techniques. X-ray diffraction patterns were obtained utilizing the PANalytical X'PERT PRO diffractometer (Cu-Kα radian, λ = 1.5418 Å, 45 kV). A Perkin-Elmer spectrum 65. Fourier-transform infrared spectroscopy (FTIR, Shimadzu FTIR-8400S) was employed in the 400 to 4,000 cm^{-1} range to characterize the shrimp co-products powder (SCP) surface groups. Sample were obtained by dispersing finely ground material in KBr powder-pressed pellets. Resulting infrared patterns helped to identify the chemical functional groups present. A scanning electron microscopy (SEM) observation was carried out using a JEOL-JSM 636O equipped with an energy-dispersive X-ray spectroscopy (EDX) system. Sample was powdered on an aluminum support previously covered with a self-adhesive pellet containing graphite. A pH meter (Bante Instruments PHS-3BW) was used to determine zero charge pH of adsorbent. UV/Vis spectrophotometer (Optizen 210UV) was employed to measure adsorbate (CR) concentrations.

2.4. Adsorption experiments

Adsorption experiments were conducted by batch. Kinetic was conducted at room temperature by mixing and shaking at 250 rpm 0.1 g of adsorbent with 100 mL of 50 mg/L solution containing CR. The flasks were shaken at intervals 0–360 min.

Isotherm was determined by shaking different amounts of adsorbent (varying from 25 to 1,000 mg) with 100 mL of 50 mg/L solution containing CR for 6 h. After shaking, 2 mL of the suspensions were centrifuged at 2,000 rpm for 2 min.

The amount of CR adsorbed was calculated based on the following equation:

$$q_e = \frac{\left(C_0 - C_e\right)V}{m} \tag{1}$$

where q_e is the amount of dye adsorbed in material, C_0 is the initial concentrations, C_e is the equilibrium concentrations of CR solutions respectively, determined by UV-Visible, V is the volume of solution containing adsorbent, m is the mass of adsorbent. The experiments were performed at the solution pH (pH 6.65) without adjustment, over the concentration range employed.

Modeling of the adsorption data was performed by non-linear regression analysis using Excel software (Solver). The suitability of this tool was assessed based on correlation coefficient (R^2) and calculation of error (sum of squares error; (SSE)) as mentioned in Eq. (2).

$$\text{SSE} = \sum_{i=1}^{n}\left(q_{\text{cal}} - q_e\right)^2 \tag{2}$$

where q_e is the experimental amount of dye adsorbed in material, q_{cal} is the calculated with model amount of dye adsorbed in material, i = test set. Kinetic data were fitted using a pseudo-first-order. Models proposed by Lagergren

[32], [Eq (3)] and pseudo-second-order model proposed by Ho and Mackay [33], [Eq (4)] were used.

$$\log\left(q_e - q_t\right) = \log q_e - \frac{K_1 t}{2.303} \tag{3}$$

$$q\left(t\right) = \frac{q_e^2 K_2 t}{1 + q_e^2 K_2 t} \tag{4}$$

where q_e, $q(t)$ are the amounts of dye adsorbed respectively, at equilibrium and at time t (mg/g) and K_1 (min^{-1}), K_2 (g/mg·min) are the adsorption rate constants for each model.

Three models were applied to determine the nature of CR sorption isotherms on SCP. The first model based on the Langmuir model [34] was represented by Eq. (5), it was based on a monolayer adsorption on the adsorbent surface, with no interaction between adsorbed molecules [35]. The second model was based on an empirical study first reported by Freundlich in 1907 [36], represented by Eq. (6) this model described the adsorption on a heterogeneous surface through a multilayer adsorption mechanism [35]. The third model reported by Redlich–Peterson [37,38] was represented by Eq. (7). This model included three adjustable parameters an empirical isotherm. This equation was widely used as a compromise between the Langmuir and Freundlich systems [38].

$$q_e = \frac{q_{\max} K_l C_e}{\left(1 + K_l C_e\right)} \tag{5}$$

$$q_e = K_F C_e^{1/n} \tag{6}$$

$$q_e = \frac{K_{\mathrm{RP}} C_e}{1 + a_R C_e^{\beta}} \tag{7}$$

where C_e is the equilibrium CR concentration (mg/L); q_e is the amount of CR adsorbed per gram of the adsorbent at equilibrium (mg/g); $q_{\max}$ is saturated monolayer adsorption capacity; K_L is Langmuir isotherm constant; K_F is the Freundlich constant [(mg/g)(L/mg)$^{1/n}$]; n is the heterogeneity factor; K_{RP} is the Redlich–Peterson adsorption capacity constant; The parameter a_R is the Redlich–Peterson isotherm constant and β is the exponent between 0 and 1.

2.5. Determination of zero-charge pH

The zero-charge pH (pH_{PZC}) of SCP was determined according to the method described in [38], by preparing 50 mL of KNO_3 solutions (10^{-2} M) and transferring to 100 mL beakers. Initial pH ($pH_{initial}$) of the solutions were adjusted in region 2–11 by addition of NaOH or HCl. Then, 0.1 g of SCP was added to the beakers. The solutions were magnetically stirred for 48 h to reach the equilibrium. The final pH was measured and the difference ($pH_{initial}$–pH_{final}) was plotted against $pH_{initial}$. The intersection points of the resulting curve with the abscissa axis, for which ΔpH = 0, gives the pH_{PZC}.

3. Results and discussion

3.1. Characterization of adsorbent

The zero-charge pH (pH_{PZC}) (Fig. 2) was determined by the point of intersection of the resulting curve with the abscissa axis, for which ΔpH = 0.

The value found was pH_{PZC} = 7.8. Therefore, the surface of the adsorbent was positively charged below pH = 7.8 and negatively charged otherwise [39].

The mechanism of uptake of CR on adsorbent could be grouped into non-electrostatic and electrostatic interactions. The adsorption capacity of the material depended on the pH of the solution and the pH_{PZC}. Knowing that the pH_{PZC} value of sample (pH_{PZC} = 7.8) was higher than the pH value of CR solution (6.65); the material is positively charged and CR was an acid dye, dissolved in water it was negatively charged. This resulted, an adsorption by electrostatic attraction between the negative charge of the anionic dye and the protonated –OH and –COOH groups on the surface of the material [40].

The XRD pattern of shrimp co-products powder is presented in Fig. 3. The diffractogram of the co-products revealed a significant amount of amorphous phase with peaks corresponding to calcite. A similar observation was reported elsewhere [30,41]. The patterns can be well fitted by the standard calcite diffraction pattern (JCPDS card no. 24-0027) [30].

The FTIR spectrum of SCP (Fig. 4) showed absorption bands assigned to symmetric stretching modes (800, 875 and 950) cm^{-1} of calcite carbonates [15,41–43]. The peak at 1,025 cm^{-1} was assigned to the C–O stretching mode [44,45]. The broad peak in the range of 1,375–1,500.53 cm^{-1} was assigned to asymmetric stretching carbonate (calcite) [42,43]. Peaks in the range of 1,300 cm^{-1} were assigned to the bending modes of the physically bonded water [46–48], Bands due to the C–H stretching vibration in the group were also observed at 2,924.18 cm^{-1} [49,50]. The small peak at 1,541.49 cm^{-1} was ascribed to the presence of protein [51,52]. The broad vibration at (3,000–3,600) cm^{-1} indicated the presence of hydroxyl and amino groups which probably originate from the chitin contained in the shrimp shells [30].

The surface morphology of co-products is shown in Fig. 5a. The SEM of powder indicated that the surface is

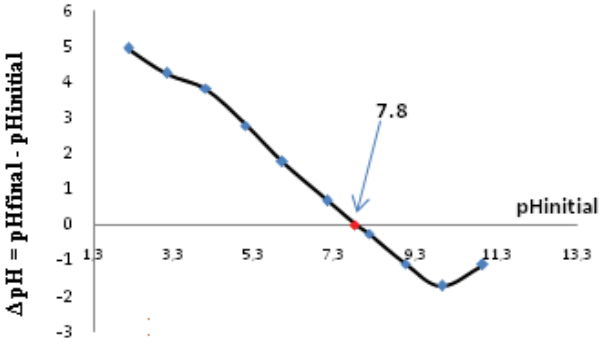

Fig. 2. Variation of the pH differential as a function of initial pH.

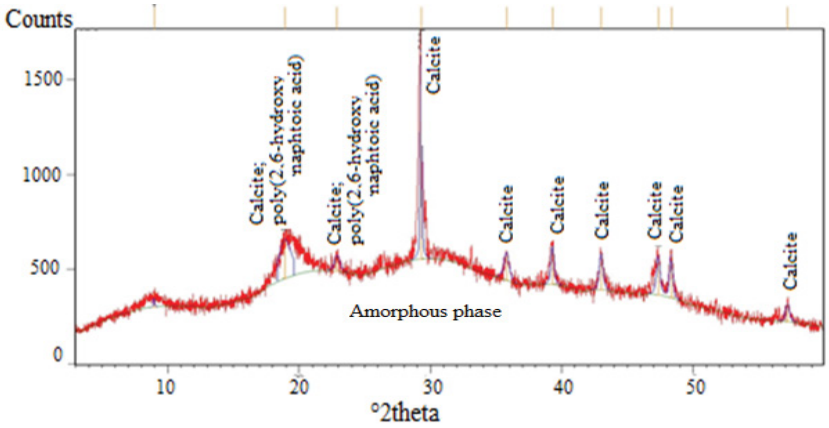

Fig. 3. X-ray diffraction pattern from shrimp co-products powder.

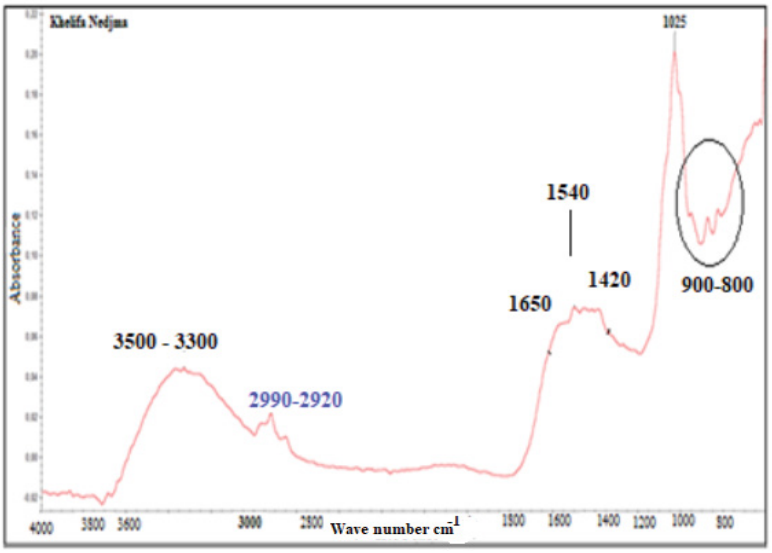

Fig. 4. FTIR spectra of SCP, circles show the calcite stretching vibration peaks.

relatively rough and contains homogeneous cavities with different geometries, which can be taken as a sign for effective adsorption of dye molecules. The EDX spectrum provided relative concentration of each element (Fig. 5b); it mainly consisted of carbon, oxygen and calcium confirming the existence of the groups C–O, C=O, C–O–C and O–H. EDX also indicated the presence of Calcite and 2,6-hydroxynaphtoic acid. Trace elements like Na, Mg, Al, Si and P were also inferred from EDX.

3.2. Results of adsorption study of CR by SCP adsorbent

Adsorption kinetics and isotherms patterns were fitted using different models including pseudo-first-order, pseudo-second-order and intra-particular diffusion models. Langmuir, Freundlich and Redlich–Peterson models were implemented using non-linear Excel Software (Solver). This method did not transform data sets; hence, no distortions were created in the original error distribution.

3.2.1. Kinetic study of the adsorption of CR by SCP adsorbent

Pseudo-first-order and pseudo-second-order kinetics, were employed to evaluate the kinetics and mechanism of solid-liquid adsorption [53,54]. Fig. 6 describes the experimental data and following adjustment using nonlinear forms of the PFO and PSO models of the adsorption of Congo red on the SCP as a function of the time.

the Table 1 grouping the results of the modeling, showed that contrary to the PFO model; the PSO model revealed a higher correlation coefficient (R^2) and a lower error calculation (SSE). Thus, the pseudo-second-order kinetic model reasonably described the mechanism of the CR adsorption by the material.

This observation supported the assumption that the adsorption was predominantly due to chemisorption [55].

Based on this work we could not be confirmed that the diffusion mechanism followed either PFO or the PSO model. For this, the kinetic results were analyzed using the intraparticular diffusion model (Fig. 7). The Weber–Morris

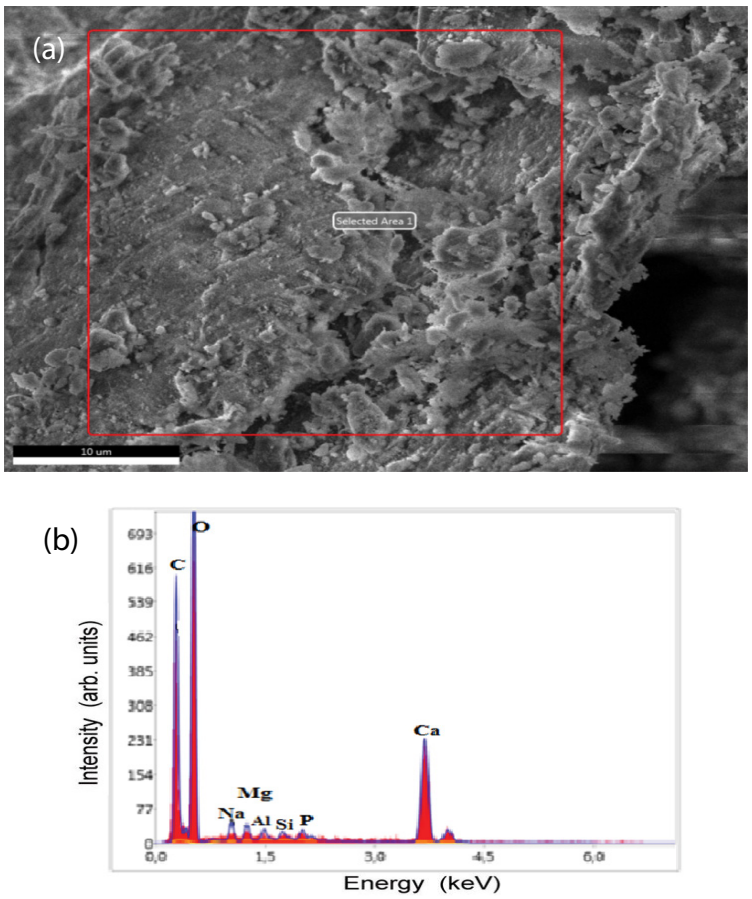

Fig. 5. SEM micrograph of shrimp co-products powder (a) and EDX spectrum (b).

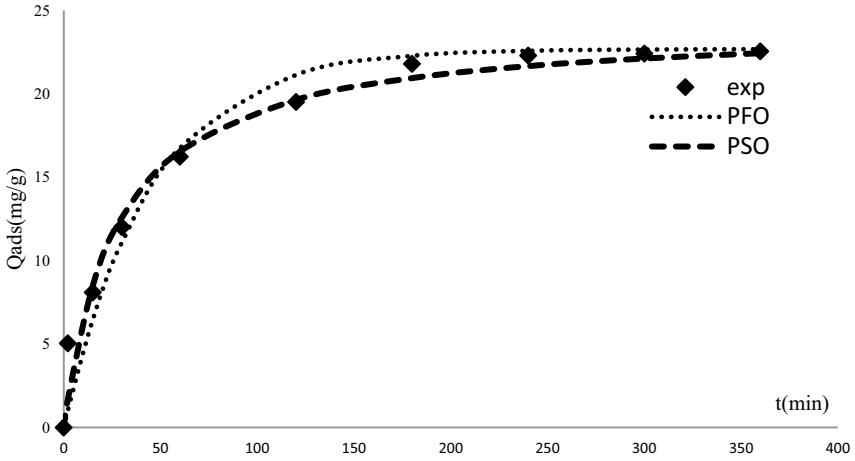

Fig. 6. Kinetic plots, pseudo-first-order and pseudo-second-order of the adsorption of CR by SCP adsorbent.

equation was used to describe the intraparticular diffusion; if the plot of q_e vs. $t^{1/2}$ was linear and passed by the origin, then the intraparticular diffusion would be the sole rate-limiting step [56]. The rate constant K_{int} is given by Eq. (8).

$$q_e = K_{int} t^{1/2} + C \quad (8)$$

where C is the intercept, C is a constant representing the boundary layer thickness, and a larger value of C represents a thicker boundary layer [57].

The constants (K_{int}) for CR were calculated and shown in Table 1. If the value of C was zero, then the rate of adsorption was controlled by intraparticle diffusion for the entire adsorption period. In the present study, the value of C was

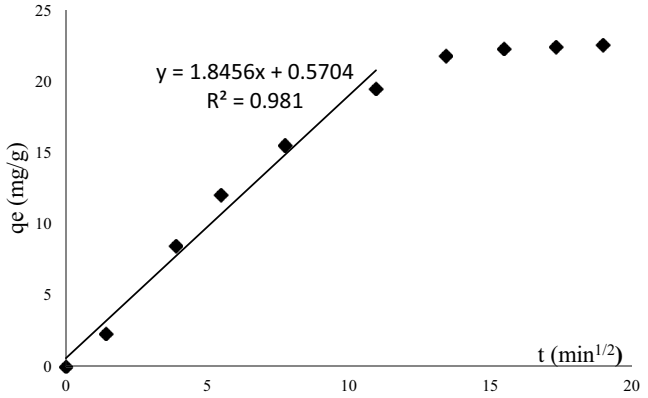

Fig. 7. Intraparticle diffusion model of the adsorption of CR by SCP adsorbent.

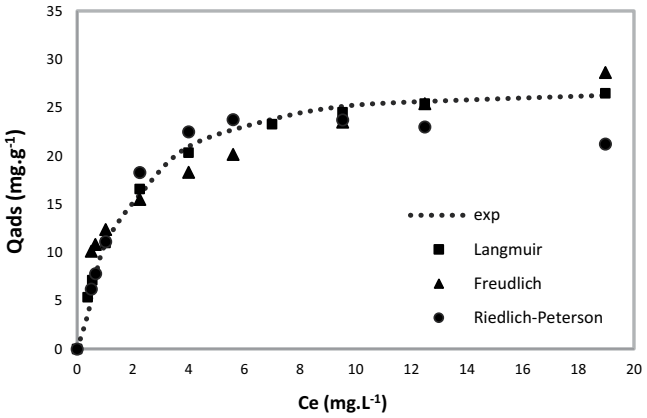

Fig. 8. Adsorption isotherm of Congo red onto SCP at 298 K.

Table 1
Kinetic parameters for the two models studied

Pseudo-first-order	Pseudo-second-order	Intraparticle diffusion
q_e (mg/g): 22.68	q_e (mg/g): 24.15	C = 0.570 (mg/g)
K_1 (g/mg·min): 0.022	K_2 (g/mg·min): 0.0015	K_{int} (g/mg·min$^{0.5}$) = 1.845
R^2: 0.9908	R^2: 0.9912	0.981
Sum: 23.3169	Sum: 1.8572	

not equal to zero. However, the plot of q_e as a function of $t^{½}$ showed more than one linear portion. As seen from Fig. 7, the plots were not linear over the whole-time range, indicating that more than one process affected the CR adsorption.

3.2.2. Isotherm of the adsorption of CR by SCP adsorbent

The adsorption isotherm models indicate how adsorbate molecules are distributed between the liquid and solid phases when the process is in the equilibrium state. This was based on analysis using Langmuir, Freundlich and Redlich–Peterson isotherms models. Analysis of the fitness between the data and different isotherm models was an important step in determining the suitable model.

The non-linear forms of the Langmuir, Freundlich and Redlich–Peterson isotherms are shown in Fig. 8 and the relevant constants are shown in Table 2. It appeared that the models of Redlich–Peterson and Langmuir were the most appropriate to describe the adsorption trends. For this, higher correlations coefficients (R^2) and the lowest error calculations (SSE) were utilized to assess the fitness of these three models. For the Freundlich model, even though the value of correlations coefficients was 0.95, the calculated error is the highest of the three, so this model did not appear to be adequate to describe the present adsorption process. Moreover, this result confirmed since the exponent β_{RP} was very close to the one (0.84), which indicated that the mathematical equations of Redlich–Peterson [Eq. (7)] and Langmuir [Eq. (5)] were similar.

It could be concluded that the experimental data collected from biosorption isotherms were better fitted to Langmuir model (i.e., a homogeneous surface containing equivalent sites and available for Congo red) [58]. According to the low values of R_L and $1/n_F$ (Table 2), that is, less than unity, the system showed favorable adsorption of CR onto SCP adsorbent. Additionally, this value of n_F (higher than 1) implied that CR dye molecules could be adsorbed with a non-parallel orientation (i.e., the adsorbate could interact with one adsorption site).

The error calculation (SSE) and correlation coefficient (R^2) for each of the equilibrium isotherm models of the adsorption process are shown in Table 2. The Freundlich and Redlich–Peterson models showed the smallest (R^2 = 0.95) and the highest (SSE), whereas the Langmuir isotherm model showed the best (R^2 = 0.99) and lowest error calculation. Thus, the isotherm that best described the adsorption behavior of the dye onto SCP was the Langmuir isotherm.

$$R_L = \frac{1}{\left(1 + K_L C_0\right)} \tag{9}$$

The value of R_L [Eq. (9)] indicates the type of isotherm to be either favorable ($0 < R_L < 1$), linear ($R_L = 1$), unfavorable ($R_L > 1$), or irreversible ($R_L = 0$). The results showed that the value of $1/n_F$ was less than unity indicating that the dye was favorably adsorbed by the adsorbent. This was in good agreement with the findings regarding to R_L values [59].

It is noticed that the maximal adsorption amount obtained from the experiment is close to the calculated value of the Langmuir model, however a margin of error occurs which is explained by the SSE error reported in Table 2.

Table 2
Isotherm parameters for different isotherm models

Langmuir	Redlich–Peterson	Freundlich
K_L (L/mg): 0.6965	K_{RP} = 13.150591	1/*n*: 0.288
q_{max} (mg/g): 28.7999	a_R = 0.5961701	K_F: 12.27
R_L: 0.0141	β_{RP} = 0.8379	
R^2: 0.998	R^2: 0.991	R^2: 0.950
SSE: 5.91	SSE: 30.37	SSE: 96.76

4. Conclusion

A new shrimp co-products-based (SCP) biosorbent was obtained via a simple route and investigated for the removal of Congo red (CR/anionic dye (acid)) from aqueous solution. The results indicated that the SCP are a promising new low-cost biosorbent. The dye kinetic study on SCP suggested that the biosorption kinetic followed the pseudo-second-order model. The isotherm data showed that the CR biosorption followed a Langmuir model. Compared to other raw biomass adsorbents (without pre-treatments), the amount adsorbed by these shells shows that SCP are effective in removing acid dyes.

Symbols

a_R	—	Redlich–Peterson isotherm constant
C_0	—	Initial concentrations of adsorbate, mg/L
C_e	—	Equilibrium concentrations of adsorbate, mg/L
C	—	Intra-particular model parameter
K_1	—	Adsorption rate constants for pseudo-first-order, g/mg·min
K_2	—	Adsorption rate constants for pseudo-second-order, g/mg·min
K_{int}	—	Intra-particular parameter
K_{RP}	—	Redlich–Peterson's adsorption capacity constant
K_L	—	Langmuir isotherm constant, L/mg
K_F	—	Freundlich constant, (mg/g)(L/mg)
m	—	Amount of adsorbent, g
n	—	Freundlich isotherm heterogeneity factor
q_e	—	Amount of pollutant adsorbed at equilibrium in material, mg/g
q_{exp}	—	Experimental amount of pollutant adsorbed in material, mg/g
q_{cal}	—	Amount calculated with model, mg/g
q_{max}	—	Monolayer adsorption capacity, mg/g
$q(t)$	—	Amounts of dye adsorbed at time *t*, mg/g
SSE	—	Sum of squares error
V	—	volume of pollutant solution, L
β	—	Redlich–Peterson exponent

References

[1] S. Zen, F.Z. El Berrichi, Adsorption of tannery anionic dyes by modified kaolin from aqueous solution, Desal. Water Treat., 57 (2016) 6024–6032.

[2] G.L.Y. Gao, M. Gao, X. Huang, D. Xu, Magnetic metal–organic frameworks in adsorption and enrichment removal of food and environmental pollutants, Crit. Rev. Anal. Chem., 50 (2020) 472–484.

[3] M.S.R. Baccar, J. Bouzid, M. Feki Blanquez, Removal of pharmaceutical compounds by activated carbon prepared from agricultural by-product, Chem. Eng. J., 211–212 (2021) 310–317.

[4] J. Rivera-Utrilla, M. Sánchez-Polo, M.Á. Ferro-García, G. Prados-Joya, R. Ocampo-Pérez, Pharmaceuticals as emerging contaminants and their removal from water. A review, Chemosphere, 93 (2013) 1268–1287.

[5] M. Boroski, A.C. Rodrigues, J.C. Garcia, L.C. Sampaio, J. Nozaki, N. Hioka, Combined electrocoagulation and TiO_2 photoassisted treatment applied to wastewater effluents from pharmaceutical and cosmetic industries, J. Hazard. Mater., 162 (2009) 448–454.

[6] M.R. Heidari, R.S. Varma, M. Ahmadian, M. Pourkhosravani, S.N. Asadzadeh, P. Karimi, M. Khatami, Photo-Fenton like catalyst system: activated carbon/$CoFe_2O_4$ nanocomposite for reactive dye removal from textile wastewater, Appl. Sci., 9 (2019) 963, doi: 10.3390/app9050963.

[7] M. Kerrou, N. Bouslamti, A. Raada, A. Elanssari, D. Mrani, M.S. Slimani, The use of sugarcane bagasse to remove the organic dyes from wastewater, J. Anal. Chem., 2021 (2021) 5570806, doi: 10.1155/2021/5570806.

[8] H. Mansour, O. Boughzala, D. Dridi, D. Barillier, L. Chekir-Ghedira, R. Mosrati, Les colorants textiles sources de contamination de l'eau: CRIBLAGE de la toxicité et des méthodes de traitement, Rev. Des Sci. De L'Eau./J. Water Sci., 24 (2011) 209–238.

[9] M.R. Narayan, Review: dye sensitized solar cells based on natural photosensitizers, Renewable Sustainable Energy Rev., 16 (2012) 208–215.

[10] H. Zhou, L. Wu, Y. Gao, T. Ma, Dye-sensitized solar cells using 20 natural dyes as sensitizers, J. Photochem. Photobiol., A, 219 (2011) 188–194.

[11] G. Calogero, J.-H. Yum, A. Sinopoli, G. Di Marco, M. Grätzel, M.K. Nazeeruddin, Anthocyanins and betalains as light-harvesting pigments for dye-sensitized solar cells, Sol. Energy, 86 (2012) 1563–1575.

[12] K. Singh, S. Arora, Removal of synthetic textile dyes from wastewaters: a critical review on present treatment technologies, Crit. Rev. Env. Sci. Technol., 41 (2011) 807–878.

[13] S. Karcher, A. Kornmüller, M. Jekel, Anion exchange resins for removal of reactive dyes from textile wastewaters, Water Res., 36 (2002) 4717–4724.

[14] H. Soonmin, Removal of dye by adsorption onto activated carbons: review, Eurasian J. Anal. Chem., 13 (2018) 332–338.

[15] N. Khelifa, J.-P. Basly, B. Hamdi, M. Baudu, Preparation of novel diatomite-based composites: applications in organic effluents sorption, Desal. Water Treat., 57 (2016) 12443–12452.

[16] A. Othmani, A. Kesraoui, M. Seffen, Removal of phenol from aqueous solution by coupling alternating current with biosorption, Environ. Sci. Pollut. Res., 28 (2021) 46488–46503.

[17] M. Naushad, T. Ahamad, Z.A. AlOthman, A.H. Al-Muhtaseb, Green and eco-friendly nanocomposite for the removal of toxic Hg(II) metal ion from aqueous environment: adsorption kinetics & isotherm modelling, J. Mol. Liq., 279 (2019) 1–8.

[18] M. Shahid, I. Shahid ul, F. Mohammad, Recent advancements in natural dye applications: a review, J. Cleaner Prod., 53 (2013) 310–331.

[19] R. Rahimian, S. Zarinabadi, A review of studies on the removal of methylene blue dye from industrial wastewater using activated carbon adsorbents made from almond bark, Prog. Chem. Biochem. Res., 3 (2020) 251–268.

[20] A.G. Varghese, S.A. Paul, M.S. Latha, Remediation of heavy metals and dyes from wastewater using cellulose-based adsorbents, Environ. Chem. Lett., 17 (2019) 867–877.

[21] D. Dahiya, P.S. Nigam, Waste management by biological approach employing natural substrates and microbial agents for the remediation of dyes' wastewater, Appl. Sci., 10 (2020) 2958, doi: 10.3390/app10082958.

[22] S.A.Y.N. Fayoud, S. Tahiri, A. Albizane, Kinetic and thermodynamic study of the adsorption of methylene blue on wood ashes, J. Mater. Environ. Sci., 6 (2015) 3295–3306.

[23] H. Wu, R. Chen, H. Du, J. Zhang, L. Shi, Y. Qin, L. Yue, J. Wang, Synthesis of activated carbon from peanut shell as dye adsorbents for wastewater treatment, Adsorpt. Sci. Technol., 37 (2019) 34–48.
[24] T.B. Cahú, S.D. Santos, A. Mendes, C.R. Córdula, S.F. Chavante, L.B. Carvalho, H.B. Nader, R.S. Bezerra, Recovery of protein, chitin, carotenoids and glycosaminoglycans from Pacific white shrimp (*Litopenaeus vannamei*) processing waste, Process Biochem., 47 (2012) 570–577.
[25] A. Abun, D. Rusmana, T. Widjastuti, K. Haetami, Prebiotics BLS from encapsulated of extract of shrimp waste bioconversion on feed supplement quality and its implication of metabolizable energy and digestibility at Indonesian local chicken, J. Appl. Anim. Res., 49 (2021) 295–303.
[26] S. Zhuang, K. Zhu, L. Xu, J. Hu, J. Wang, Adsorption of Co^{2+} and Sr^{2+} in aqueous solution by a novel fibrous chitosan biosorbent, Sci. Total Environ., 825 (2022) 153998, doi: 10.1016/j.scitotenv.2022.153998.
[27] B. Turan, G. Sarigol, P. Demircivi, Adsorption of tetracycline antibiotics using metal and clay embedded cross-linked chitosan, Mater. Chem. Phys., 279 (2022) 125781, doi: 10.1016/j.matchemphys.2022.125781.
[28] Y. Saharan, J. Singh, R. Goyat, A. Umar, H. Algadi, A.A. Ibrahim, R. Kumar, S. Baskoutas, Nanoporous and hydrophobic new chitosan-silica blend aerogels for enhanced oil adsorption capacity, J. Cleaner Prod., 351 (2022) 131247, doi: 10.1016/j.jclepro.2022.131247.
[29] A.C. Sadiq, A. Olasupo, W.S.W. Ngah, N.Y. Rahim, F.B.M. Suah, A decade development in the application of chitosan-based materials for dye adsorption: a short review, Int. J. Biol. Macromol., 191 (2021) 1151–1163.
[30] Y. Zhou, L. Ge, N. Fan, M. Xia, Adsorption of Congo red from aqueous solution onto shrimp shell powder, Adsorpt. Sci. Technol., 36 (2018) 1310–1330.
[31] A. Kumar, R. Singh, S. Kumar Upadhyay Sanjay Kumar, M.U. Charaya, Biosorption: the removal of toxic dyes from industrial effluent using phytobiomass – a review, Plant Arch., 21 (2021) 1320–1325.
[32] S. Lagergren, Zur theorie der sogenannten adsorption gelˆster stoffe, Kungliga SvenskaVetenskapsakademiens, Handlingar, 24 (1898) 1–39.
[33] Y.S. Ho, G. McKay, Pseudo-second-order model for sorption processes, Process Biochem., 34 (1999) 451–465.
[34] I. Langmuir, The constitution and fundamental properties of solids and liquids. Part I. solids, J. Am. Chem. Soc., 38 (1916) 2221–2295.
[35] S. Hosseini, M.A. Khan, M.R. Malekbala, W. Cheah, T.S.Y. Choong, Carbon coated monolith, a mesoporous material for the removal of methyl orange from aqueous phase: adsorption and desorption studies, Chem. Eng. J., 171 (2011) 1124–1131.
[36] H. Freundlich, Über die Adsorption in Lösungen, Z. Phys. Chem., 57U (1907) 385–470.
[37] O. Redlich, D.L. Peterson, A useful adsorption isotherm, J. Phys. Chem., 63 (1959) 1024–1024.
[38] N.T.R.N. Kumara, N. Hamdan, M.I. Petra, K.U. Tennakoon, P. Ekanayake, Equilibrium isotherm studies of adsorption of pigments extracted from kuduk-kuduk (*Melastoma malabathricum* L.) pulp onto TiO_2 nanoparticles, J. Chem., 2014 (2014) 468975, doi: 10.1155/2014/468975.
[39] M. Kosmulski, The pH-dependent surface charging and points of zero charge: V. Update, J. Colloid Interface Sci., 353 (2011) 1–15.
[40] V. Vimonses, S. Lei, B. Jin, C.W.K. Chow, C. Saint, Adsorption of Congo red by three Australian kaolins, Appl. Clay Sci., 43 (2009) 465–472.
[41] R. Li, W. Liang, J.J. Wang, L.A. Gaston, D. Huang, H. Huang, S. Lei, M.K. Awasthi, B. Zhou, R. Xiao, Z. Zhang, Facilitative capture of As(V), Pb(II) and methylene blue from aqueous solutions with MgO hybrid sponge-like carbonaceous composite derived from sugarcane leafy trash, J. Environ. Manage., 212 (2018) 77–87.
[42] S. Amin, R.P. Rastogi, M.G. Chaubey, K. Jain, J. Divecha, C. Desai, D. Madamwar, Degradation and toxicity analysis of a reactive textile diazo dye-direct red 81 by newly isolated *Bacillus* sp. DMS2, Front. Microbiol., 11 (2020) 576680, doi: 10.3389/fmicb.2020.576680.
[43] S. Gunasekaran, G. Anbalagan, S. Pandi, Raman and infrared spectra of carbonates of calcite structure, J. Raman Spectrosc., 37 (2006) 892–899.
[44] E.M. Nese Ertugay, Adsorption isotherm, kinetic, and thermodynamic studies for methylene blue from aqueous solution by needles of *Pinus Sylvestris* L., Pol. J. Environ. Stud., 23 (2014) 1995–2006.
[45] T.M. Hafshejani, W. Wang, J. Heggemann, A. Nefedov, S. Heissler, Y. Wang, P. Rahe, P. Thissen, C. Wöll, CO adsorption on the calcite (10.4) surface: a combined experimental and theoretical study, Phys. Chem. Chem. Phys., 23 (2021) 7696–7702.
[46] M. Belhachemi, F. Addoun, Comparative adsorption isotherms and modeling of methylene blue onto activated carbons, Appl. Water Sci., 1 (2011) 111–117.
[47] P. Lura, F. Winnefeld, X. Fang, A simple method for determining the total amount of physically and chemically bound water of different cements, J. Therm. Anal. Calorim., 130 (2017) 653–660.
[48] L. Song, J. Yu, H. Xie, R. Zhang, Y. Xue, C. Xue, Physical properties and conformational changes of shrimp surimi from *Litopenaeus vannamei* during cold gelation, LWT, 153 (2022) 112516, doi: 10.1016/j.lwt.2021.112516.
[49] I. Laaz, M.-J. Stébé, A. Benhamou, D. Zoubir, J.-L. Blin, Influence of porosity and surface modification on the adsorption of both cationic and anionic dyes, Colloids Surf., A, 490 (2016) 30–40.
[50] X. Peng, L.L. Ye, C.H. Wang, H. Zhou, B. Sun, Temperature- and duration-dependent rice straw-derived biochar: characteristics and its effects on soil properties of an ultisol in southern China, Soil Tillage Res., 112 (2011) 159–166.
[51] M. Kousha, S. Tavakoli, E. Daneshvar, A. Vazirzadeh, A. Bhatnagar, Central composite design optimization of Acid Blue 25 dye biosorption using shrimp shell biomass, J. Mol. Liq., 207 (2015) 266–273.
[52] J. Majtán, K. Bíliková, O. Markovič, J. Gróf, G. Kogan, J. Šimúth, Isolation and characterization of chitin from bumblebee (*Bombus terrestris*), Int. J. Biol. Macromol., 40 (2007) 237–241.
[53] H. Liu, X. Cai, Y. Wang, J. Chen, Adsorption mechanism-based screening of cyclodextrin polymers for adsorption and separation of pesticides from water, Water Res., 45 (2011) 3499–3511.
[54] G. Yang, L. Wu, Q. Xian, F. Shen, J. Wu, Y. Zhang, Removal of Congo red and Methylene blue from aqueous solutions by vermicompost-derived biochars, PLoS One, 11 (2016) e0154562, doi: 10.1371/journal.pone.0154562.
[55] G.F. Malash, M.I. El-Khaiary, Methylene blue adsorption by the waste of Abu-Tartour phosphate rock, J. Colloid Interface Sci., 348 (2010) 537–545.
[56] J. Wang, X. Guo, Adsorption kinetic models: physical meanings, applications, and solving methods, J. Hazard. Mater., 390 (2020) 122156, doi: 10.1016/j.jhazmat.2020.122156.
[57] Y.H. Magdy, H. Altaher, Kinetic analysis of the adsorption of dyes from high strength wastewater on cement kiln dust, J. Environ. Chem. Eng., 6 (2018) 834–841.
[58] I. El Saliby, L. Erdei, J.-H. Kim, H.K. Shon, Adsorption and photocatalytic degradation of methylene blue over hydrogen–titanate nanofibres produced by a peroxide method, Water Res., 47 (2013) 4115–4125.
[59] Z. Belala, M. Jeguirim, M. Belhachemi, F. Addoun, G. Trouvé, Biosorption of basic dye from aqueous solutions by date stones and palm-trees waste: kinetic, equilibrium and thermodynamic studies, Desalination, 271 (2011) 80–87.